Available online at www.sciencedirect.com

ScienceDirect

Geochimica et Cosmochimica Acta 212 (2017) 1–15

Geochimica et Cosmochimica Acta

www.elsevier.com/locate/gca

Effects of complexation between organic matter (OM) and clay mineral on OM pyrolysis

Hongling Bu [a,b], Peng Yuan [a,*], Hongmei Liu [a], Dong Liu [a], Jinzhong Liu [c], Hongping He [a], Junming Zhou [a,b], Hongzhe Song [a,b], Zhaohui Li [d]

[a] *CAS Key Laboratory of Mineralogy and Metallogeny/Guangdong Provincial Key Laboratory of Mineral Physics and Materials, Guangzhou Institute of Geochemistry, Chinese Academy of Sciences, Guangzhou 510640, China*

[b] *University of Chinese Academy of Sciences, Beijing 100049, China*

[c] *State Key Laboratory of Organic Geochemistry, Guangzhou Institute of Geochemistry, Chinese Academy of Sciences, Guangzhou 510640, China*

[d] *Geosciences Department, University of Wisconsin-Parkside, Kenosha, WI 53144, USA*

Received 15 November 2016; accepted in revised form 9 April 2017; available online 30 May 2017

Abstract

The stability and persistence of organic matter (OM) in source rocks are of great significance for hydrocarbon generation and the global carbon cycle. Clay-OM associations commonly occur in sedimentation and diagenesis processes and can influence the pyrolytic behaviors of OM. In this study, clay-OM complexes, i.e., interlayer clay-OM complexes and clay-OM mixture, were prepared and exposed to high-pressure pyrolysis conditions in confined gold capsule reactors to assess variations in OM pyrolysis products in the presence of clay minerals. Three model organic compounds, octadecanoic acid (OA), octadecy trimethyl ammonium bromide (OTAB), and octadecylamine (ODA), were employed and montmorillonite (Mt) was selected as the representative clay mineral. The solid acidity of Mt plays a key role in affecting the amount and composition of the pyrolysis gases generated by the clay-OM complexes. The Brønsted acid sites significantly promote the cracking of hydrocarbons through a carbocation mechanism and the isomerization of normal hydrocarbons. The Lewis acid sites are primarily involved in the decarboxylation reaction during pyrolysis and are responsible for CO_2 generation. Mt exhibits either a catalysis effect or pyrolysis-inhibiting during pyrolysis of a given OM depending on the nature of the model organic compound and the nature of the clay-OM complexation. The amounts of C_{1-5} hydrocarbons and CO_2 that are released from the Mt-OA and Mt-ODA complexes were higher than those of the parent OA and ODA, respectively, indicating a catalysis effect of Mt. In contrast, the amount of C_{1-5} hydrocarbons produced from the pyrolysis of Mt-OTAB complexes was lower than that of OTAB, which we attribute to an inhibiting effect of Mt. This pyrolysis-inhibiting effect works through the Hoffmann elimination that is promoted by the catalysis of the Brønsted acid sites of Mt, therefore releasing smaller amounts of gas hydrocarbons than the nucleophilic reaction that is induced by the halide ions in OTAB. In particular, the interlayer space of Mt acts as an 'amplifier' that magnifies the above-mentioned catalysis or pyrolysis-inhibiting effect, due to the greater number of Brønsted acid sites with high acidity in the interlayer space. These findings are potentially important for understanding the storage and transfer mechanisms of natural OM in sedimentation and diagenesis processes.

Keywords: Organic matter; Montmorillonite; Pyrolysis; Hydrocarbon; Solid acidity; Clay-organic complex

* Corresponding author. Fax: +86 20 85290341.
E-mail address: yuanpeng@gig.ac.cn (P. Yuan).

http://dx.doi.org/10.1016/j.gca.2017.04.045
0016-7037/

1. INTRODUCTION

The associations between organic matters (OM) and clay minerals in sediments or sedimentary rocks have been attracting increasing research interest in past decades (Ransom et al., 1998; Ingalls et al., 2004; Mayer, 2004; Lopez-Sangil and Rovira, 2013; Zhu et al., 2016). Multiple independent studies have shown the widespread existence of clay-OM associations, for instance, OM in sediments or source rocks is primarily associated with clay minerals (Bergamaschi et al., 1997; Mayer, 1999), and separating OM from clay minerals by physical methods (e.g., lateral transport fractionation technology) is difficult (Keil et al., 1994; Mayer, 1994). In particular, a direct proportionality between the concentration of OM and the sediment mineral surface area (MSA) was observed. This observation supports clay-OM association because the MSA of sediment is actually controlled by the abundance of the clay minerals with very high specific surface area (such as smectite), which has two orders of magnitude greater MSA than quartz or carbonate (Hedges and Keil, 1995). As proposed by these studies, the mechanisms of OM preservation and enrichment with clay minerals constitute a key factor that affects the global carbon cycle processes such as hydrocarbon-generation.

Several types of clay-OM associations have been proposed including: (i) the physical sheltering (e.g., encapsulation) of OM by clay mineral aggregates (Ransom et al., 1998; Salmon et al., 2000); (ii) the sorption of OM by clay minerals (Kell et al., 1994; Keil and Cowie, 1999; Satterberg et al., 2003; Zimmerman et al., 2004); and (iii) the intercalation of OM within the interlayer space of swelling clay minerals (e.g., smectite group minerals) (Kennedy et al., 2002; Zhu et al., 2016), which is actually a kind of sorption but only occurs in the interlayer space of clay. The resultant from the third clay-OM association has been termed "organo-clay nanocomposite" because the intercalation occurs at the nanometer or even angstrom scale (Theng et al., 1986; Kennedy et al., 2002; Kennedy and Wagner, 2011).

The storage of OM within the interlayer space of clay minerals has been investigated less often than the other two types of clay-OM associations (physical sheltering and sorption of OM by clay minerals). Because OM intercalation occurs at very small scales, characterizing the resulting complexes of this clay-OM association (hereafter denoted as "interlayer clay-OM complex") is technically challenging. A few previous studies had focused on the occurrence and characteristic of natural interlayer clay-OM complexes in some source rocks or sediments (Perez Rodriguez et al., 1977; Theng et al., 1986; Schulten et al., 1996; Lu et al., 1999; Zhu et al., 2016), in which the intercalation of natural organics was indicated by the expansion of the interlayer distance of montmorillonite (Mt) or mixed-layered Mt-Illite. The understanding of interlayer clay-OM complexes got further improved by Kennedy, who conducted a series of related studies on thermally immature Cretaceous sediments from the western interior seaway of North America (Kennedy et al., 2002) and the Deep Ivorian Basin of the eastern Atlantic (Kennedy et al., 2002; Kennedy and Wagner, 2011). The above-mentioned studies clearly demonstrated that expandable smectite plays a key role in the preservation of OM and the intercalation of OM in swelling clay plays an important role in OM accumulation in the geological record. Recently, Kennedy et al. (2014) further characterized interlayer clay-OM complexes by using high-resolution transmission electron microscopy (HRTEM) and obtained direct HRTEM evidences of occurrence of OM as nanometer-scale intercalations in swelling clays.

However, the geochemical behavior of interlayer organics in interlayer clay-OM complexes currently remains poorly understood, although this topic is actually of great meaning not only for understanding the storage mechanism of organic carbon in sedimentary records but also for knowing the pathways of interlayer organics that are involved in the global carbon cycle. Moreover, this topic is beneficial to understanding the role and behavior of clay minerals in organic geological processes. Among the most urgent issues in this field, the thermal stability and the pyrolytic behaviors of interlayer organics are of particular interest because they directly reflect the pathways and mechanisms regarding how the interlayer organics enter the geologic record or the hydrocarbon-generation process by their thermal degradation to small organic molecules.

In fact, the pyrolysis of organics and hydrocarbon generation in the presence of clay minerals (e.g., Kuhl, 1942; Jurg and Eisma, 1964; Faure et al., 2003; Li et al., 2003; Berthonneau et al., 2016) have been explored since as early as 1940s; however, interlayer clay-OM complexes had never been taken into account, because the occurrence of interlayer clay-OM complexes had not even been recognized. In most experimental studies on the pyrolysis of organics in the presence of clay minerals, natural organics (such as kerogen and bitumen) were simply mixed with clay minerals to create clay-OM mixture (e.g., Galwey, 1972; Heller-Kallai et al., 1984; Tannenbaum and Kaplan, 1985a; Pan et al., 2010; Hu et al., 2014), and interlayer clay-OM complexes had not been purposely prepared. Thus, how the intercalation complexation between OM and clay minerals could affect the pyrolytic behaviors of OM remains largely unknown, so related investigations need to be conducted.

In this work, the high temperature-pressure pyrolytic behavior of clay-OM complexes is studied. Three aliphatic hydrocarbons, octadecanoic acid ($CH_3(CH_2)_{16}COOH$, abbreviated as OA), octadecy trimethyl ammonium bromide ($CH_3(CH_2)_{17}N(CH_3)_3Br$, OTAB), and octadecylamine ($CH_3(CH_2)_{16}CH_2NH_2$, ODA) were used as the model organic compounds that were complexed with Mt. Mt is a ubiquitously occurring swelling clay minerals in source rocks and sediments, and it possesses expandable interlayer space for hosting intercalations of organics. The reason for selecting the above organics is as follows. Aliphatic hydrocarbons are an important lipid fraction in living organisms and appear as a common organic constituent of source rocks (Xiang et al., 1997; Thiel et al., 1999). In particular, aliphatic hydrocarbon (such as fatty acids) represents one of the most commonly occurring natural organics during hydrocarbon generation of source rocks (Vandenbroucke and Largeau, 2007), although a thorough

understanding on the highly complex composition and structure of kerogen and bitumen in source rocks has not yet been achieved (Bousige et al., 2016). The decarboxylation and subsequent cracking of aliphatic hydrocarbons are assumed to serve as key processes for petroleum generation (Jurg and Eisma, 1964; Shimoyama and Johns, 1971). It is also found that aliphatic hydrocarbons exist in the interlayer space of clay minerals in natural clay-OM complexes in sediments (Schulten et al., 1996; Zhu et al., 2016). Among the model organic compounds, OA is one of the most abundant fatty acids in nature; OTAB and ODA are selected for comparison purposes, because they have the same alkyl chains as that of OA but with different functional groups. Moreover, alkyl chains and ammonium ions are typical groups of natural organics in source rocks (Krooss et al., 1995; Vandenbroucke and Largeau, 2007). A comparison based on the difference of functional groups is expected to be useful in revealing the influences of the characteristics of organics on the pyrolytic behaviors of clay-OM complexes. In addition, based on the knowledge of intercalation chemistry of clay minerals (Bergaya and Lagaly, 2013), either OTAB or ODA can be readily cationized and thus can be intercalated into the interlayer of Mt via cation exchange to prepare interlayer clay-OM complexes; in contrast, OA is non-ionic so that it cannot be intercalated into the interlayer of Mt. With this comparison, some information about the different roles of the interlayer space and external surface of clay minerals in the pyrolysis of OM can be obtained. Anhydrous conditions (i.e., no extra water was added) was applied in the pyrolysis experiments to exclude the effects of water as much as possible, aiming at simplifying the possible factors and thus only focus on the effects of clay-OM complexation on the pyrolysis. A confined high temperature-pressure system and its associated gas chromatograph were used to quantitatively monitor the details of pyrolytic reactions. The structural characteristics of the interlayer clay-OM complexes were studied by using X-ray diffraction (XRD) and Fourier transform infrared (FTIR) techniques to comprehensively investigate the clay-OM complexation and the OM pyrolysis mechanisms.

2. MATERIALS AND METHODS

2.1. Materials and Mt-OM complexes preparation

OA (with a purity of 95 wt%), OTAB (98 wt%), and ODA (99 wt%) were purchased by Sigma-Aldrich and were used without further purification. The raw Mt sample (sourced from Inner Mongolia, China) was purified by repeated sedimentation to remove impurities, and a <2 μm fraction was collected and used for the experiments. The chemical compositions (wt%) of Mt are as follows: SiO_2, 63.0%; Al_2O_3, 16.2%; Fe_2O_3, 4.9%; CaO, 0.3%; MgO, 4.6%; Na_2O, 3.6%; K_2O, 0.1%; TiO_2, 0.4%; Ignition Loss, 6.9%. The cation exchange capacity (CEC) of the Mt is 110.5 mmol/100 g. According to X-ray diffraction (XRD) analysis, the content of Mt in the specimen is high (>90%) and a small amount of quartz impurity exists in Mt. Before being used for clay-OM complexation, Mt was Na-saturated by three Na-saturation/washing cycles. The procedure was as follows. The Mt powder was dispersed in deionized water and treated with 0.5 M NaCl solution under vigorous stirring at 80 °C for 24 h. The resultant solid was separated by centrifugation and the product was again sent for treating with NaCl solution, and the above process was repeated three times. The product was repeatedly washed with distilled water and then freeze-dried for 48 h.

The interlayer Mt-OTAB complex was prepared by dispersing a known amount of organics (4.34 g) in distilled water, stirring at 80 °C for 30 min, and slowly adding 20 g of Mt, with a mass ratio of water/Mt of 20:1. The mixture was stirred for 12 h at 60 °C. The interlayer Mt-ODA complex was prepared according to the following procedure. 5.96 g of ODA was added to 200 mL of 0.14 M HCl solution and kept at 80 °C by using a water bath. The resulting solution was added to a dispersion that consisted of 10 g of Mt and 1000 mL of distilled water. The mixture was stirred at 80 °C for 30 min. The solids of the above-mentioned mixtures were filtered and repeatedly washed with distilled water to remove OTAB or ODA in excess and then were dried and ground. The resulting interlayer Mt-OTAB and Mt-ODA complexes are labeled as Mt_{inter}-OTAB and Mt_{inter}-ODA, respectively. The contents of organic matter in Mt_{inter}-OTAB and Mt_{inter}-ODA were 30.3 wt% and 36.4 wt%, respectively. The Mt-OM mixtures were prepared by using previously reported methods (Espitalie et al., 1980; Tannenbaum and Kaplan, 1985a; Wei et al., 2006; Hu et al., 2014), in which the organics were simply mixed with clay minerals by grinding, and the mass ratio of clay/OM also refers to these previous studies. 5 g of Mt and 1.25 g of model organics, OA, OTAB, and ODA, were mixed and ground through ball milling for 20 min to achieve a uniform and complete mixing by using a Pulverisette-6 Planetary Mill. The products are denoted as Mt-OA, Mt-OTAB and Mt-ODA, respectively. The content of organic matter in the Mt-OM mixture (Mt-OA, Mt-OTAB or Mt-ODA) was 20.0 wt%.

2.2. Characterization of Mt-OM complexes

The content of organic matter in the interlayer Mt-OM complex was determined by elemental analyses, which were performed by using an Elementar Vario EL III Universal CHN elemental analyzer. Major element oxides were determined by using a Rigaku RIX 2000 X-ray fluorescence spectrometer (XRF) on fused glass beads. The powder XRD analysis was performed on a Bruker D8 Advance diffractometer with a Ni filter and Cu Kα radiation (40 kV and 40 mA). The diffraction patterns were collected from 2° to 40° (2θ) at a scanning rate of 3° min^{-1}. The FTIR spectra of the samples in the pressed KBr pellets were recorded on a Bruker Vertex-70 FTIR spectrometer. The spectra were collected over a range of 400–4000 cm^{-1} with 64 scans at a resolution of 4 cm^{-1}. A thermogravimetric (TG) analysis of the samples was performed using a Netzsch 449C instrument. Approximately 5–10 mg of samples powder was heated at a heating rate of 10 °C/min under a high-purity N_2 atmosphere (60 cm^3/min).

The measurements on the solid acidity of Mt were performed by using Hammett indicators method (Liu et al., 2011). The types of solid acid sites were differentiated by using diffuse reflectance Fourier transform infrared spectroscopy (DRIFT) in which pyridine was used as a probe molecule. The detailed measurement procedures are described in Part I of Supplementary Materials (SM).

2.3. Pyrolysis experiment

The high temperature-pressure pyrolysis experiment was conducted in a flexible gold capsule (6 mm outside diameter, 0.25 mm wall thickness and 6 cm length) that was contained within a steel pressure vessel (autoclave). The vessel was placed in a furnace with a fan at the bottom to maintain a stable temperature during the experiment. One end of the gold capsule was welded before being loaded with the sample. After the samples were loaded, the open end of each capsule was squeezed in a vise under argon purging to create an initial seal. The sealed capsule was then welded under an argon atmosphere. During the welding, the previously welded end was submerged in cold water to prevent the reactant from heating. The experimental system allowed twelve pressure vessels to be placed in a single furnace, and one gold capsule was placed into each vessel. The internal pressure of the vessel was adjusted to 36 MPa by pumping water into the vessels before heating. The error of the pressure measurements was $<\pm 0.1$ MPa. The internal pressure was automatically maintained during the pyrolysis experiment by pumping water into or out of the vessel. The pyrolysis experiment was conducted at 350 °C, which was fixed by a thermocouple placed in the furnace and attached to one of the vessels. The error of the temperature measurements was $<\pm 1$ °C. The initial heating to 350 °C was achieved in approximately 24 h, and the subsequent isothermal heating lasted for 48 h. The amount of the loaded OM was approximately 100 mg, and that of the Mt-OM complex was approximately 300 mg.

The volatile components generated from the pyrolysis experiments were released by piercing the capsule and then were collected and concentrated in a device connected to an Agilent 6890N gas chromatograph (GC) that was modified with Wasson-ECE Instrumentation. The modified GC was equipped with three detectors: a flame ionization detector (FID) was used to analyze gaseous hydrocarbons (carrier gas: helium); a thermal conductivity detector (TCD) was used to analyze H_2 (carrier gas: nitrogen); and another TCD was used to analyze other inorganic gases (using helium as a carrier gas). The tests based on the external standard gases indicated that the relative errors of this device were less than 0.5%. The main operating steps were as follows: First, the entire device was evacuated by a vacuum pump to reach an internal pressure ($<1 \times 10^{-2}$ Pa). Then, the gold capsule was pierced with a needle to allow the gases to escape into the device, and the modified GC was opened to let the gases enter until the internal pressure reached a stable value. Finally, the gas components were analyzed in an automatically controlled procedure for the GC device. The oven temperature for the hydrocarbon gas analysis was initially held at 70 °C for 6 min, increased from 70 to 130 °C at 15 °C/min, and increased again from 130 to 180 °C at 25 °C/min, and then held at 180 °C for 2 min. The temperature was held at 90 °C for the inorganic gas analysis.

3. RESULTS

3.1. Structural characteristics of the Mt-OM complexes

The XRD patterns of the Mt and Mt-OM complexes are shown in Fig. 1. The (001) characteristic diffraction of Mt appears at approximately 7° (2θ) with d_{001} value of 1.26 nm (Fig. 1a). In the XRD patterns of the two interlayer Mt-OM complexes, Mt_{inter}-OTAB and Mt_{inter}-ODA (Fig. 1d and f), the d_{001} values are 2.36 nm and 3.34 nm, respectively. These d_{001} values correspond to interlayer distances of approximately 1.40 nm and 2.38 nm, respectively. The reason is that the height of a tetrahedron-octahedron-tetrahedron (TOT) layer of montmorillonite is approximately 0.96 nm (Yariv et al., 2011; Bergaya and Lagaly, 2013), and the interlayer distance of Mt is obtained by subtracting the thickness of TOT from the d_{001} value. The interlayer distances of Mt_{inter}-OTAB and Mt_{inter}-ODA are obviously larger than that of Mt (approximately 0.30 nm), indicating the successful intercalation of OTAB and ODA into the interlayer space of Mt. A diffraction peak at 5° with a d spacing of 1.77 nm is shown for Mt_{inter}-ODA (Fig. 1f). It is assigned to (002) reflection, suggesting that the intercalation of OM occurred without the destruction of the layered structure of Mt. The positions of the (001) diffractions of the Mt-OM mixtures (Mt-OA, Mt-OTAB and Mt-ODA) do not obviously shift (Fig. 1b, c, and e), compared to that of the (001) diffraction of Mt, which indicates the non-intercalation states of the OMs in the Mt-OM mixtures. It is noteworthy that a broadening of the (001) reflection in the case of Mt-ODA (Fig. 1e) is observed. This broadening implies irregular basal spacing and therefore a low crystalline order of Mt. A possible reason of the broadening is the very small-scale intercalation of ODA during sample preparation, but such intercalation (if exists) is negligible because the position of (001) reflection of Mt-ODA are entirely close to that of Mt. In addition, for all Mt-OM complexes, the intensities of the characteristic non-basal (02,11) reflections (hk-band groups) of Mt at approximately 20° (2θ) remain unchanged, reflecting that the layered structure of Mt was not disturbed during samples preparation.

The FTIR spectra of Mt, OMs and Mt-OM complexes are shown in Fig. 2. The assignments for the vibrations are summarized in Table 1, and they are based on the previous reports (Madejova and Komadel, 2001; Andjelkovic et al., 2006; Yuan et al., 2008; Pálková et al., 2010). The FTIR spectra of the Mt-OM mixtures show a combination of characteristic bands of Mt and of the OMs (OA, OTAB and ODA) (Fig. 2a–c, e, g–i; Table 1). However, both Mt_{inter}-OTAB and Mt_{inter}-ODA exhibit some vibrations that are different from those of Mt (Fig. 2a, d, f). For example, the broad band at 3440 cm^{-1} is attributed to O—H stretching vibrations of the physically adsorbed water and interlayer water, which are strongly affected by the OM intercalation (He et al., 2004). For Mt_{inter}-OTAB

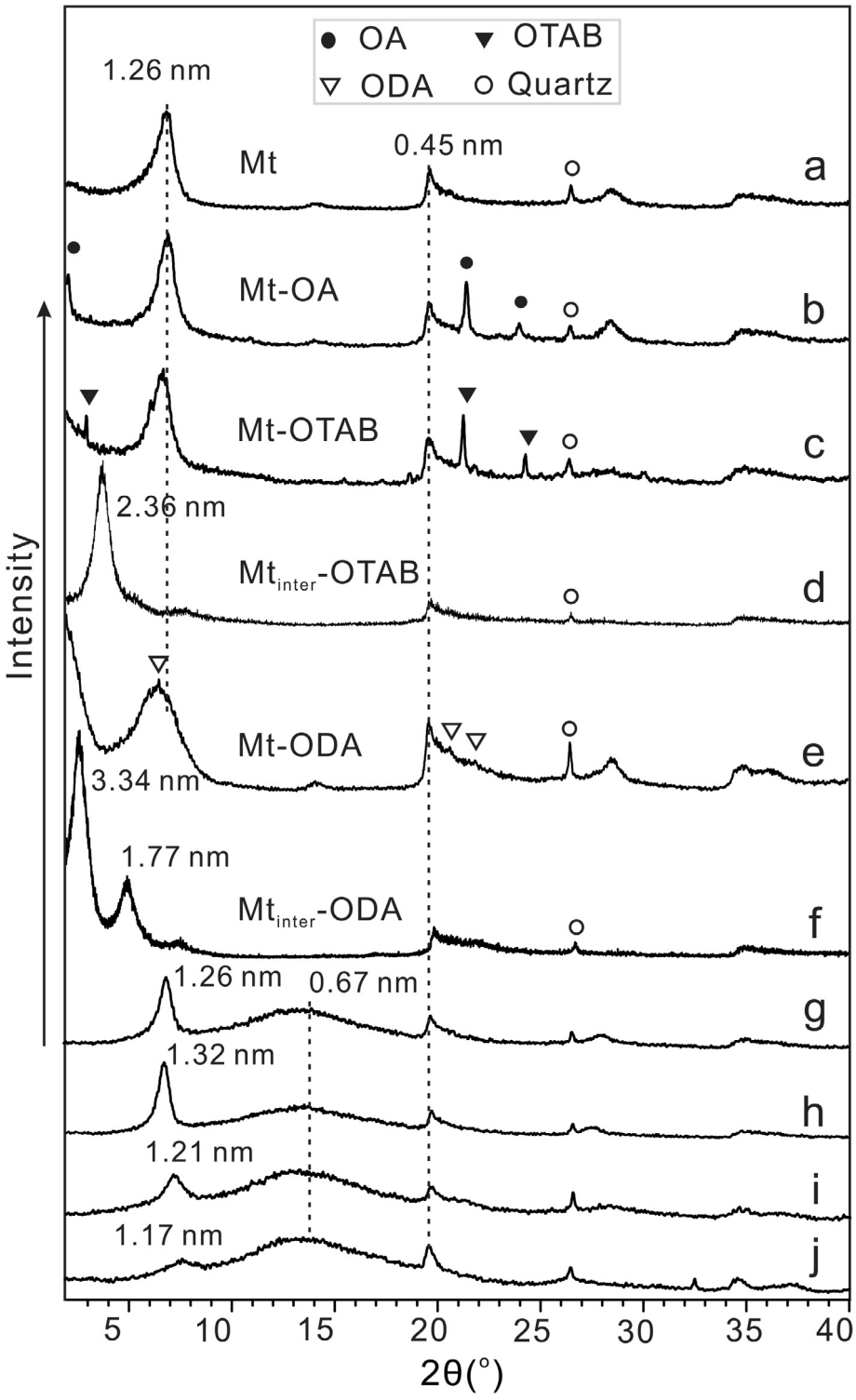

Fig. 1. Powder X-ray diffraction patterns of the clay-OM complexes and the solid residues reclaimed from the pyrolysis. (a) Mt; (b) Mt-OA; (c) Mt-OTAB; (d) Mt_{inter}-OTAB; (e) Mt-ODA; (f) Mt_{inter}-ODA; (g) the solid residue reclaimed from the pyrolysis of Mt-OTAB; (h) The solid residue from Mt_{inter}-OTAB pyrolysis; (i) the solid residue from Mt-ODA pyrolysis; (j) the solid residue from Mt_{inter}-ODA pyrolysis.

(Fig. 2d), the intensity of 3440 cm^{-1} band is obviously reduced and the band position shifts to a lower wavenumber, indicating the occurrence of OTAB intercalation. For Mt_{inter}-ODA (Fig. 2f), the 3440 cm^{-1} band almost disappears, which implies that the ion-exchange in this case was relatively complete. These observations indicate that the interlayer water was largely removed through organics intercalation (Ma et al., 2010; Karaca et al., 2013). The

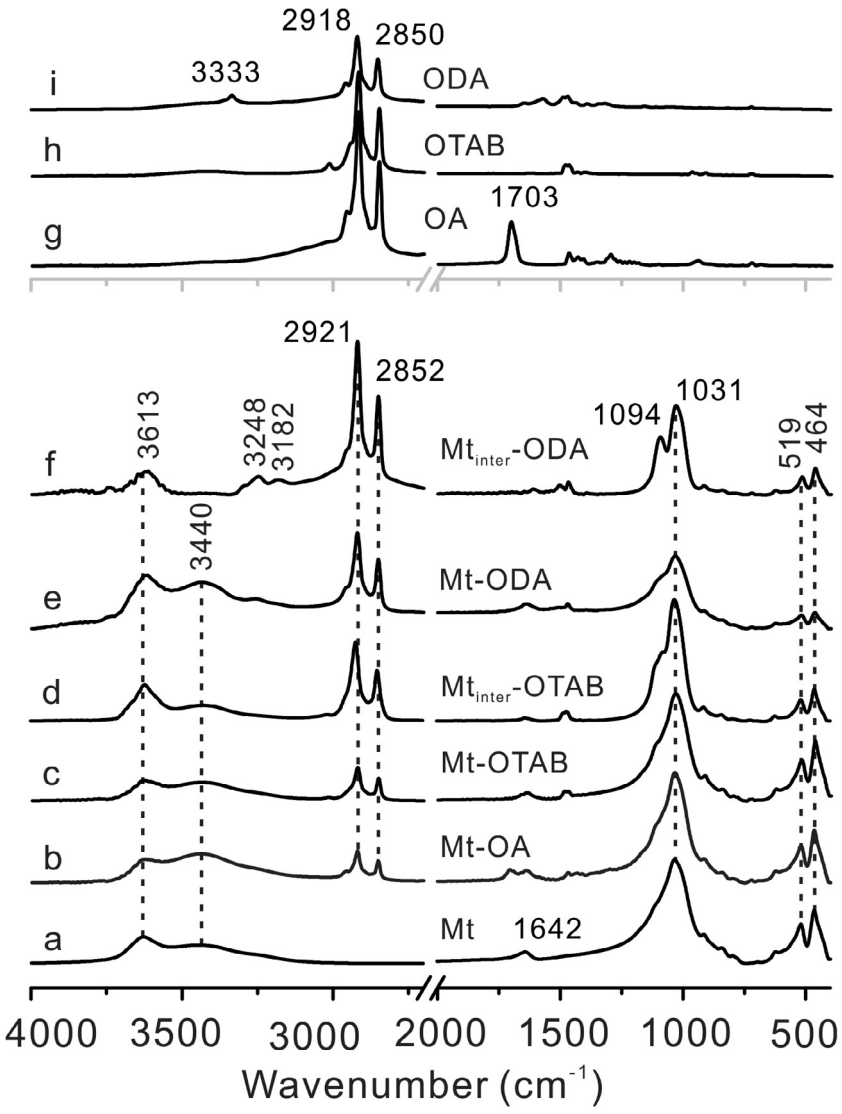

Fig. 2. FTIR spectra of clay, model organics, and clay-OM complexes. (a) Mt; (b) Mt-OA; (c) Mt-OTAB; (d) Mt_{inter}-OTAB; (e) Mt-ODA; (f) Mt_{inter}-ODA; (g) OA; (h) OTAB; (i) ODA.

Table 1
Band assignments of the FTIR spectra of the samples (Madejova and Komadel, 2001; Andjelkovic et al., 2006; Yuan et al., 2008; Pálková et al., 2010).

Wavenumber (cm^{-1})	Band assignments
3613	O—H stretching of structural hydroxyl group of Mt
3440	O—H stretching of water of Mt
3333	N—H stretching
3248/3182	N—H asymmetrical stretching
2921/2918	CH_2 antisymmetric stretching
2852/2850	CH_2 symmetric stretching
1703	C=O stretching
1642	H—O—H bending
1094	Perpendicular Si—O stretching
1031	Si—O stretching
519	Si—O—Al deformation
464	Si—O—Si bending

amounts of the remaining water in Mt_{inter}-OTAB and Mt_{inter}-ODA, determined by the mass loss up to 200 °C in the TG curves (not shown), are 2.88% and 0.55%, respectively. In addition, for the interlayer Mt-OM complexes (Fig. 2d and f), the Si—O stretching vibration of Mt at approximately 1031 cm^{-1} splits into a sharp band at 1031 cm^{-1} with a shoulder around 1094 cm^{-1} (attributed to perpendicular Si—O stretching; Slosiariková et al., 1992). The above-mentioned phenomenon confirms the intercalation of OTAB or ODA into the interlayer space of Mt via cation exchange, which is in agreement with the XRD results.

3.2. Gaseous components produced from the pyrolysis of Mt-OM complexes

3.2.1. Methane and total gaseous hydrocarbon (ΣC_{1-5})

The amounts of gaseous hydrocarbon produced from pyrolysis are shown in Fig. 3 (the detailed data is given as

Table S3 in Part II of SM). The amount of methane generated from OTAB pyrolysis is 45.13 mg/g of OM, which is almost two orders of magnitude higher than that from OA pyrolysis (Fig. 3a). The methane amount for Mt-OA is higher than that for OA, and the methane amounts for Mt-ODA and Mt_{inter}-ODA are close to that for ODA. Nevertheless, the methane amounts for the Mt-OTAB complexes are generally lower than that for OTAB alone; especially, the methane amount for Mt_{inter}-OTAB (5.92 mg/g of OM) is significantly lower than that for OTAB and that for Mt-OTAB (20.03 mg/g of OM). The amount of methane released from OTAB pyrolysis is approximately 7 times as large as that from Mt_{inter}-OTAB (Fig. 3a).

The amounts of total gaseous hydrocarbons (ΣC_{1-5}) produced from OM pyrolysis almost have the same trend as the amounts of methane (Fig. 3a). The ΣC_{1-5} value of OA is 0.99 mg/g of OM, which is lower than that of Mt-OA. The ΣC_{1-5} value of ODA is 0.58 mg/g of OM, nearly equivalent to that of Mt-ODA. The ΣC_{1-5} value of Mt_{inter}-ODA is approximately 10 times as large as that of ODA. The ΣC_{1-5} value of OTAB is 60.43 mg/g of OM, which is obviously higher than that of Mt-OTAB (24.14 mg/g of OM) and is much higher than that of Mt_{inter}-OTAB (10.63 mg/g of OM).

3.2.2. Non-hydrocarbon gases

The amounts of H_2 produced from the pyrolysis of OA, Mt-OA, OTAB, and Mt-OTAB are all very low (Fig. 3b). The H_2 yield for ODA is much higher than that for OA or OTAB, and is nearly equivalent to that for Mt-ODA; however, the H_2 yield for Mt_{inter}-ODA is almost negligible (Fig. 3b).

The amount of CO_2 that released from OA pyrolysis is 17.18 mg/g of OM (Fig. 3c), lower than that from Mt-OA pyrolysis (21.94 mg/g of OM). For OTAB, the amount of produced CO_2 is low (1.27 mg/g of OM), whereas the amount of CO_2 released from Mt-OTAB is 18.83 mg/g of OM, which is approximately 2 times greater than that from Mt_{inter}-OTAB (8.71 mg/g of OM). Almost no CO_2 was released from ODA, whereas the amount of CO_2 produced from Mt-ODA reaches 15.65 mg/g of OM, which is approximately 8 times as large as that from Mt_{inter}-ODA (1.85 mg/g of OM) (Fig. 3c).

3.2.3. Ratios of iso-alkanes/n-alkanes and alkenes/alkanes

The isomerization in the pyrolysis of OA alone was very limited, because the ratios of *i*-butane/*n*-butane (iC_4/nC_4) and *i*-pentane/*n*-pentane (iC_5/nC_5) for OA are only 0.01 and 0.03, respectively. For Mt-OA, these two ratios significantly increased to 0.25 (iC_4/nC_4) and 0.57 (iC_5/nC_5) (Fig. 3d). For OTAB, the ratios of iC_4/nC_4 and iC_5/nC_5 vary with the clay-OM associations. The variation trend of the iC_4/nC_4 and iC_5/nC_5 ratios follows an order of Mt_{inter}-OTAB > OTAB > Mt-OTAB. For ODA, the isomerization was promoted in the pyrolysis of Mt-ODA complexes, especially for Mt_{inter}-ODA. The ratios of iC_4/nC_4 and iC_5/nC_5 are significantly higher than those of ODA and of Mt-ODA (Fig. 3d).

Only trace amounts of C_2H_4 and C_3H_6 were produced during the pyrolysis of OA, OTAB and ODA (Fig. 3e). However, for all OM, both the C_2H_4/C_2H_6 and $C_3H_6/$

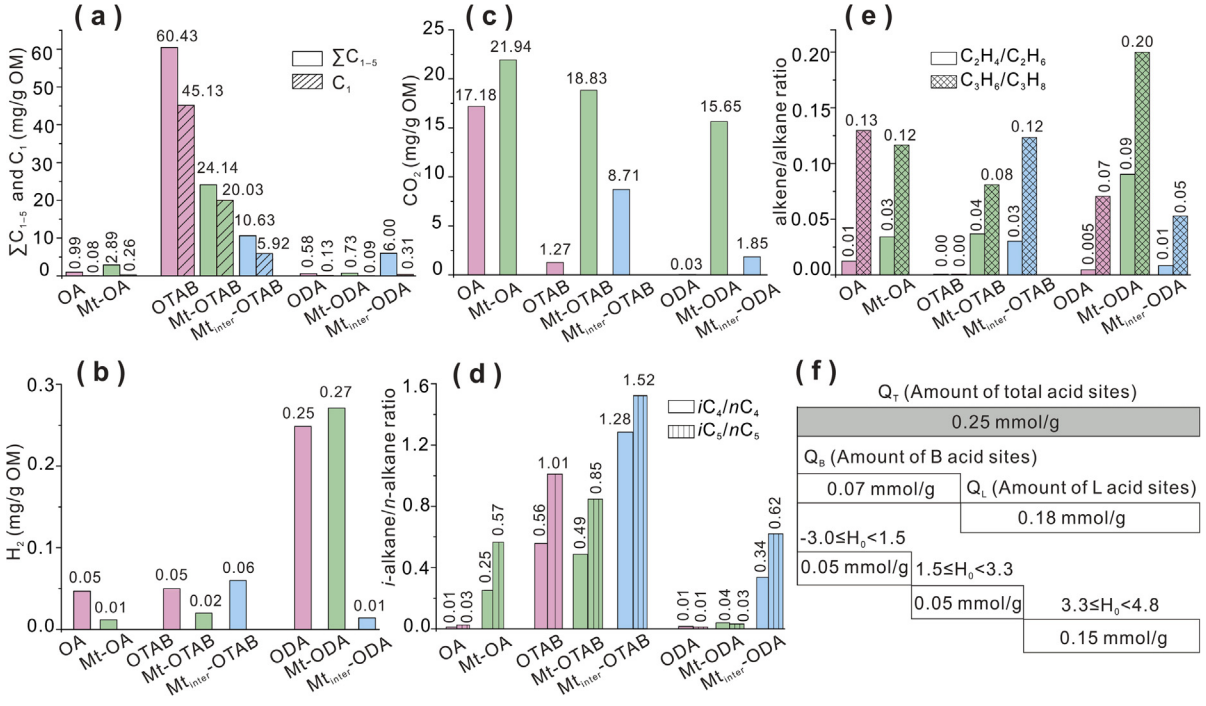

Fig. 3. Variations of the amount and composition of the gaseous pyrolysis products of different clay-OM complexes. (a) Amounts of total gaseous hydrocarbons (ΣC_{1-5}) and methane (C_1); (b) amounts of H_2; (c) amounts of CO_2; (d) ratios of iso-alkanes/*n*-alkanes; (e) ratios of alkenes/alkanes; (f) amounts of solid acid sites of Mt. Q_T: the amount of total acid sites; Q_B: the amount of Brønsted acid sites; Q_L: the amount of Lewis acid sites; H_0 denotes the solid acid strength determined by Hammett indicators method.

C_3H_8 ratios are higher for the Mt-OM complexes than for OM alone. The C_2H_4/C_2H_6 and C_3H_6/C_3H_8 ratios of Mt_{inter}-OTAB are close to those of Mt-OTAB (Fig. 3e). However, the C_2H_4/C_2H_6 and C_3H_6/C_3H_8 ratios for the Mt-ODA are higher than those of Mt_{inter}-ODA. In addition, both ratios for ODA are very low, similar to the case of Mt_{inter}-ODA (Fig. 3e).

4. DISCUSSION

4.1. Influence of Mt-OM complexation on yield of hydrocarbons

The much higher yield of C_{1-5} hydrocarbons from Mt-OA than from OA indicates that OA complexation with Mt obviously affected the pyrolysis of OA, especially promoted the production of low-molecular-mass hydrocarbons. As demonstrated by previous studies, clay minerals with inherent solid acidity may participate in the pyrolysis reactions of organics (Singh et al., 2007; Bergaya and Lagaly, 2013; Liu et al., 2013). Some studies that focused on hydrocarbon generation from natural kerogen also indicated that the hydrocarbon proportions of gas in the pyrolysis products increased as kerogen was mixed with Mt (Tannenbaum and Kaplan, 1985a; Huizinga et al., 1987a; Kumar et al., 1995; Pan et al., 2010). The present experimental results of Mt-OA are in agreement with the previous findings.

Mt_{inter}-ODA represents a case that is different from those of Mt-OA and of previous studies, in which only the external surface of Mt was considered (Huizinga et al., 1987a, 1987b; Pan et al., 2010). Much higher yield of C_{1-5} hydrocarbons from Mt_{inter}-ODA than that from Mt-ODA is shown. This result is due to the different occurrence of solid acidity in the interlayer space and in the external surface of Mt, and it implies that the catalytic sites for the pyrolysis mainly arose from the interlayer space of Mt.

These interlayer catalytic sites likely source from the interlayer hydrated cations, which is one of the primary Brønsted acidity (i.e., proton-donating capability; shorted as B acidity hereafter) of Mt (Frenkel, 1974; Newman, 1987; Tyagi et al., 2006). According to the XRF analysis result (Table S4 in part III of SM), the Na_2O contents in Mt_{inter}–OTAB and Mt_{inter}–ODA are 0.2 wt% and 0.5 wt %, respectively; and they are obviously lower than that of Mt (3.6 wt%). This result indicates that a small quantity of Na^+ remained in the interlayer space of Mt_{inter}–OTAB and Mt_{inter}–ODA, although most interlayer Na^+ of Mt had been exchanged by the organics. The water molecules associated with the remaining interlayer Na^+ very likely acted as B acid sites because they were strongly dissociated and capable of providing protons. Theng (1971) indicated that as smectite was expanded with more than a single molecular layer of water, the polarization effect of the interlayer cation would be distributed among a large number of water molecules, and the effective acidity in such a system would approach that of water in an aqueous solution. In contrast, at low water contents, the polarization forces would become more concentrated on the few residual water molecules, significantly increasing their dissociation and proton-donating ability. The dissociation constant of the residual water may be on the order of 10^6 times higher than that of normal water (Fripiat and Cruz-Cumplido, 1974). Therefore, the water molecules associated with the remaining interlayer Na^+ ions of Mt acted as the B acid sites, which initiated the hydrocarbon cracking of ODA through a carbocation pathway (Tannenbaum and Kaplan, 1985b; Kissin, 1987).

From the perspective of the surface chemistry of clay minerals, there are several possible sources of solid acid sites (schematically represented in Fig. 4) of Mt. Besides the interlayer dissociated water described above, the silanol (Si—OH) and aluminol (Al—OH_2OH) groups at the edge surface of Mt are also intrinsic B acid sites due to their high pK_a values. A detailed subdivision on these types of B acid sites have been achieved by Liu et al. (2013, 2014, 2015a, 2015b) and Tournassat et al. (2016), who used the first principles molecular dynamics (FPMD) model to simulate the surface acidity of clay minerals. In addition, possible B acid sites also include the H_3O^+ ions electrostatically captured by the negatively charged basal surface, in which the negative charge are sourced from element substitution (e.g., Si—Al substitution in Si—O tetrahedron) (Newman, 1987; Rupert et al., 1987). The Lewis (L) acid sites mainly arise from the octahedrally coordinated Al^{3+} and/or Fe^{3+} ions exposed at the edges of Mt crystallites (Newman, 1987; Rupert et al., 1987). According to the solid acidity measurement results (Fig. 3f), the amounts of B and L acid sites of Mt at the pyrolysis temperature (350 °C) are 0.07 mmol/g and 0.18 mmol/g, respectively. This result indicates that the solid acidity of Mt still works for the pyrolysis of OM under high-temperature pyrolysis conditions. For Mt-OA and Mt-ODA, the organics were not intercalated into the interlayer so that they were mostly catalyzed by the acid sites at the external surface, which resulted in a relatively low yield of C_{1-5} hydrocarbons. However, the amount of C_{1-5} hydrocarbons produced from Mt_{inter}-ODA is approximately 8 times greater than that from Mt-ODA, indicating the more significant catalytic effect of the interlayer B acid sites than of the B acid sites at the external surface for the yield of gaseous hydrocarbons. This result could be due to two possible reasons: (i) one is that the interlayer B acid sites are with high acidity, as proposed in previous reports aforementioned; (ii) the other is, because of the low proportion of the edge surface relative to the interlayer inner surface (Macht et al., 2011), the number of interlayer B acid sites is much larger than that of B acid sites at the external surface.

Contrary to the case of the Mt-ODA complexes, the yield of C_{1-5} hydrocarbons from the Mt-OTAB complexes is much lower than that from OTAB alone. In particular, Mt_{inter}-OTAB produced the lowest amount of gaseous hydrocarbons. It appears that the aforementioned catalytic effect of Mt applicable to the case of Mt-ODA complexation was inhibited or counteracted in the case of Mt-OTAB complexation. This result is due to the nature of OTAB and the catalysis of the B acid sites. The main compositional difference of OTAB compared to OA and ODA is the presence of halide anions in OTAB structure. During the pyrolysis of quaternary ammonium, halide anions are

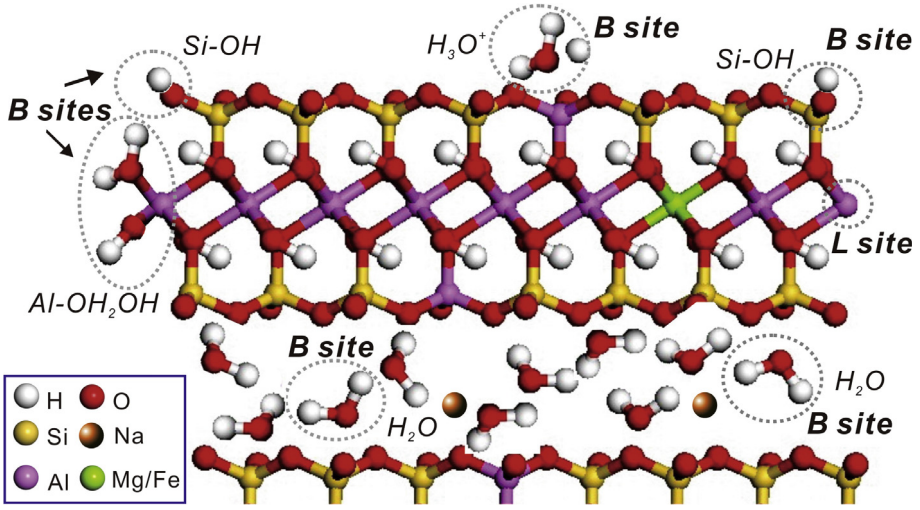

Fig. 4. Schematic representation of the possible sources of solid acid sites of Mt. *B* site denotes the Brønsted acid site; *L* site denotes the Lewis acid site.

susceptible to attack methyl at elevated temperatures (Cui et al., 2008). For the pyrolysis of molecular OTAB (pure OTAB or OTAB in Mt-OTAB), nucleophilic substitution on the R_4N^+ moiety by a bromine ion led to the formation of R—Br and tertiary amine (Fig. 5a). In contrast, for the pyrolysis of ionic OTAB (i.e., OTA^+ in Mt_{inter}-OTAB), bromine ions were absent, so the Hoffmann elimination reaction was promoted through the breaking of C—N bond by the catalysis of the B acid sites of Mt (Rajagopal et al., 1992; Liu et al., 2013), producing an olefin and a tertiary amine (such as trimethylamine) (Fig. 5b) (Xie et al., 2001; Davis et al., 2004; Bellucci et al., 2007; Cui et al., 2008). It is noteworthy that, the configuration of OTA^+ in the interlayer of Mt could also affect the pathways of pyrolysis; however, understanding the interlayer OTA^+ configuration needs a detailed computational simulation (e.g., molecular dynamics simulation; Liu et al., 2007) and is beyond the scope of this work. According to the aforementioned experimental results, the nucleophilic substitution reaction released greater amounts of low-molecular-mass hydrocarbons than the Hoffmann elimination reaction. OTAB produced the highest amount of C_{1-5} hydrocarbons, among the three OTAB-involved samples, due to that its pyrolysis followed the nucleophilic substitution reaction pathway; Mt_{inter}-OTAB produced the lowest amount of C_{1-5} hydrocarbons, due to that the OTAB pyrolysis in it mainly decomposed through a Hoffmann elimination reaction by the catalysis of B acid sites in the interlayer space of Mt. The C_{1-5} hydrocarbons production of Mt-OTAB exhibited as an intermediate state between OTAB and Mt_{inter}-OTAB, because both nucleophilic substitution and Hoffmann elimination happened in this case. This result implies that Mt played as an inhibiter for the hydrocarbon production in the pyrolysis of halide-bearing OM; this pyrolysis-inhibiting effect was realized through the Hoffmann elimination that was promoted by the catalysis of the B acid sites of Mt.

The XRD patterns of the solid residues reclaimed from the pyrolysis experiments confirm the difference of the Mt-OM complexes. As shown in Fig. 1(g–j), a broad diffraction with a *d* spacing of approximately 0.67 nm is shown in the XRD patterns of all solid residues. It is ascribed to the non-gaseous amorphous products generated from the pyrolysis of Mt-OM complexes, and its appearance clearly indicates the occurrence the pyrolysis of OM. The d_{001} values of the solid residues of both Mt-OTAB (Fig. 1g) and Mt-ODA (Fig. 1i) are close to the d_{001} value of Mt, indicating the interlayer space did not undergo obvious disturbance during pyrolysis. However, Mt_{inter}-ODA and Mt_{inter}-OTAB show obvious difference in their XRD patterns of the solid pyrolysis residues. The solid residue of Mt_{inter}-ODA exhibits a weak (001) diffraction with a *d* spacing of 1.17 nm (Fig. 1j), indicating that most interlayer organics had been decomposed into gaseous hydrocarbon or solid products that had left the interlayer space, thus largely reducing the interlayer distance. In contrast, the solid residue of Mt_{inter}-OTAB exhibits a distinct (001) diffraction with a *d* spacing of 1.32 nm (Fig. 1h), indicating the survival of some interlayer organics after the pyrolysis of interlayer OTAB. These results are in good agreement with the pyrolysis results and provide additional evidences for the catalysis effect (i.e., pyrolysis-promoting effect) of Mt in the case of the Mt-ODA complexes and the pyrolysis-inhibiting effect of Mt in the case of the Mt-OTAB complexes.

4.2. Influence of Mt-OM complexation on isomerization, alkene–alkane conversion and decarboxylation

Isomerization, alkene–alkane conversion and decarboxylation are among the most important reactions in petroleum generation. Isomerization represents a process that affects the branched and normal hydrocarbons in source rocks, which has been investigated extensively. Several possible factors may affect the relative concentration of branched and normal hydrocarbons in natural environments (Tannenbaum and Kaplan, 1985b), such as the type of OM and catalysis in clay-rich rocks. In this study, the larger *i*-alkanes/*n*-alkanes ratios for the interlayer Mt-OM

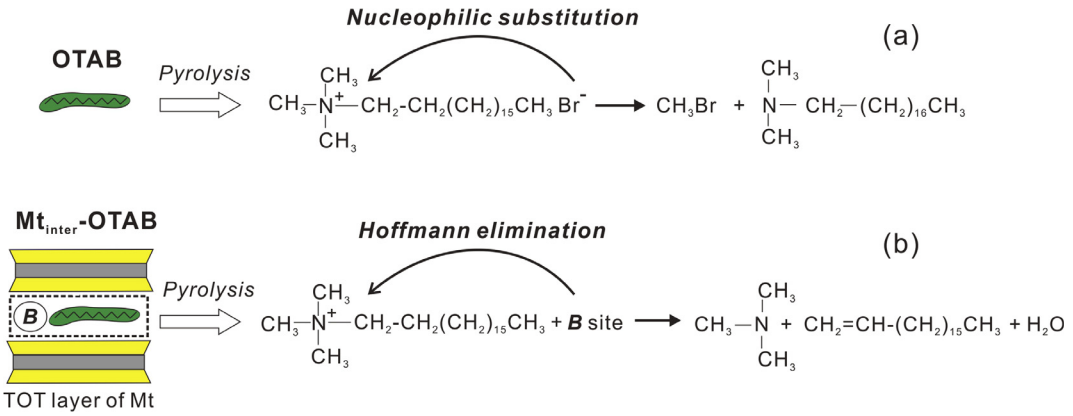

Fig. 5. Schematic representation of the processes of: (a) Nucleophilic substitution reaction in the pyrolysis of OTAB alone; (b) Hoffmann elimination reaction in the pyrolysis of Mt_{inter}-OTAB. TOT denotes tetrahedron-octahedron-tetrahedron. *B* or *B* sites denotes the Brønsted acid site.

complexes (i.e., Mt_{inter}-OTAB and Mt_{inter}-ODA) than for OM alone (Fig. 3d) indicates that isomerization in the thermally induced cracking of OM was promoted as OM occurred in the interlayer of Mt. This phenomenon is attributed to the promotion of isomerization via the carbocation mechanism, which is associated with the B acid sites in the interlayer of Mt. For OM alone, its cracking follows the free radical mechanism (Johns, 1979); however, in the presence of B acid catalyst (such as Mt), the cracking of OM adopts a carbonium ion pathway, since B acid sites provide protons to initiate the formation of carbocations (Greensfelder et al., 1949; Johns, 1979; Kissin, 1987). As mentioned earlier, the residual water in the interlayer of Mt acted as B acid sites with strong acidity, so it catalyzed the carbocation reaction and significantly enhanced isomerization as well as the yield of *i*-alkanes. This catalytic effect is much less obvious for the Mt-OM mixtures (Mt-OTAB and Mt-ODA) than for the interlayer Mt-OM complexes (Fig. 3d). The reason is that the primarily B acid sites for Mt-OM mixture came from the silanol and aluminol groups at the external surface of Mt particles (Liu et al., 2013; Tournassat et al., 2016), and the amounts of these B acid sites were lower than that of interlayer B acid sites. Moreover, the isomerization in the case of Mt-OA is much more distinct than the cases of Mt-ODA and slightly weaker than the case of Mt-OTAB (Fig. 3d), which implies that the isomerization in the pyrolysis of Mt-OM mixture is also highly relevant to the characteristics of the OM itself.

The alkene–alkane conversion is indicated by the alkenes/alkanes ratios. A low yield of ethylene and propene may occur if the produced gas olefins are unstable and are readily transformed to saturated hydrocarbons during the pyrolysis of aliphatic hydrocarbons. For the pyrolysis products of the Mt-OM mixtures, the C_2H_4/C_2H_6 and C_3H_6/C_3H_8 ratios are higher than those of OM alone (Fig. 3e). Similar observation was reported by Pan et al. (2010), whose study shown higher C_2H_4/C_2H_6 and C_3H_6/C_3H_8 ratios for oil plus Mt than for oil alone. However, lower olefins/alkanes ratios for kerogen plus Mt than kerogen alone or kerogen plus calcite (or dolomite) were also observed in some previous studies (Tannenbaum and Kaplan, 1985a, 1985b; Pan et al., 2008), suggesting the complexity of the nature clay-OM reactions. For the interlayer Mt-OM complexes, the OM characteristics appeared as an important factor affecting the alkenes/alkanes ratio. In the case of Mt-OTAB complexes, the amount of produced alkenes is slightly higher for Mt_{inter}-OTAB than that for Mt-OTAB (Fig. 3e), which might result from the aforementioned effect of interlayer B acid sites for the promotion of the cleavage of C—N bonds and the Hoffmann elimination (Rajagopal et al., 1992; Scaffaro et al., 2009). However, in the case of Mt-ODA complexes, much higher C_2H_4/C_2H_6 and C_3H_6/C_3H_8 ratios for Mt-ODA than those for Mt_{inter}-ODA is shown (Fig. 3e). Meanwhile, the amount of produced H_2 for Mt_{inter}-ODA is largely lower than those for ODA or Mt-ODA (Fig. 3b). The H_2 production seems to be independent on Mt because considerable amount of H_2 was released from the pyrolysis of ODA regardless of the presence or absence of Mt (Fig. 3b), whereas the H_2 production was decreased to almost zero in the case of Mt_{inter}-ODA. This result suggests that H_2 was very likely engaged in the hydrogenation reaction in the case of Mt_{inter}-ODA, and the alkenes were mostly transformed to saturated hydrocarbons so that much lower alkene/alkane ratios for Mt_{inter}-ODA than for Mt-ODA were obtained. Previous studies have also reported the influence of H_2 production on hydrogenation and the alkene/alkane ratios (Qader and Hill, 1969; Mango, 1996), although why a large amount of H_2 was produced from pure ODA remains unclear.

The decarboxylation reaction is particularly important for fatty acids, because it results in the removal of the carboxyl group and the release of CO_2 and gaseous hydrocarbons. The amounts of CO_2 produced from OA and Mt-OA are highly relevant to the decarboxylation reaction. The lower CO_2 yield from OA than that from Mt-OA indicates that Mt promoted the decarboxylation of OA. And this effect was realized by the L acid sites that resulted from the Al^{3+} and/or Fe^{3+} ions exposed along the edges of smectite particles (Alomon and Johns, 1975; Newman, 1987). The role of L acid site in catalyzing decarboxylation has been well documented, and they were found to be able to

extract electrons from the acylate ions to form acylate radical intermediates, which then promoted the formation of alkyl radicals through rearrangement and gave rise to the loss of CO_2 (Solomon, 1968; Galwey, 1970; Johns and Shimoyama, 1972). As shown in Fig. 3c, a small amount of CO_2 was released from the pyrolysis of OTAB and ODA, although either of them does not contain carboxyl group. This result is attributed to the reaction between water and organics in high-temperature pyrolysis conditions, which could produce CO_2 and gaseous hydrocarbon such as CH_4 (Hoering, 1984; Lewan, 1997; Seewald et al., 1998; Seewald, 2003; Pan et al., 2010). For OTAB or ODA alone, the amount of the physically adsorbed water at the surface of organics is small, so the produced CO_2 is minor. In contrast, in the case of Mt-OTAB or Mt-ODA, considerable amount of physically adsorbed water existed at the external surface of Mt because of the hydrophilic nature of clay. The introduction of these water molecules into the high-temperature pyrolysis systems significantly enhanced the above-mentioned water-organics reaction and thus led to much higher CO_2 yield than that in the case of OM pyrolysis in the absence of clay. Similarly, the CO_2 yields from Mt_{inter}-OTAB and Mt_{inter}-ODA are substantially higher than OTAB and ODA, respectively, and this result is due to the existence of interlayer water of Mt. However, this effect is not as distinct as the case of Mt-OM mixtures, since the amount of interlayer water is smaller than that of the physically adsorbed water at the external surface of Mt.

The above-mentioned results demonstrate that isomerization, alkene–alkane conversion and decarboxylation reactions during the pyrolysis of OM are closely related to the presence of clay minerals. The solid acid sites of clay minerals play an important role in these reactions. B acid sites can provide protons to initiate hydrocarbon cracking through a carbocation mechanism for the pyrolysis of long-chain aliphatic hydrocarbons and promote alkene–alkane conversion through hydrogenation. L acid sites from the edges of clay minerals mainly contribute to the decarboxylation and therefore the generation of CO_2 during the pyrolysis of fatty acids. Other factors, such as the characteristics of OM, the physically adsorbed water and the produced gases (e.g., H_2), also influence the amounts and composition of the gaseous hydrocarbons products. All factors should be taken into account for given pyrolysis systems in assessing the actual hydrocarbon-generation mechanisms.

4.3. Implication of clay-OM complexation for hydrocarbon generation in natural systems

The present pyrolysis experiments demonstrate that the way of clay-OM complexation and the nature of OM or clay minerals are the key factors that determine the hydrocarbon generation of clay-OM complexes. Of particular interest is that, the pyrolysis-inhibiting effect of clay for some clay-OM complexes (e.g., Mt-OTAB and Mt_{inter}-OTAB) was observed. This phenomenon is contrary to the pyrolysis-promoting of organics in the presence of clay minerals, which had been generally reported since as early as 1940s (Kuhl, 1942; Faure et al., 2003; Li et al., 2003; Berthonneau et al., 2016) and was also observed in this work (for the Mt-ODA complexes). Therefore, the occurrence of the pyrolysis-inhibiting effect by clay implies the complexity of OM pyrolysis in argillaceous source rocks is even higher than that was already known. It can be anticipated that, in natural pyrolysis systems, the actual performance (e.g., pyrolysis-inhibiting or pyrolysis-promoting) of clay minerals should be integratedly influenced by the above-mentioned factors.

Our results also indicate the importance of clay-OM complexation on affecting not only the quantity of hydrocarbons generation, but also the types and composition of the produced hydrocarbons by controlling the isomerization, alkene–alkane conversion and decarboxylation reactions. For example, some studies have reported different concentrations of branched hydrocarbons in various crude oils and considerable variations in the ratio of branched to normal hydrocarbons with the depth and the maturation of the associated source rocks (Thompson, 1979, 2016; Hunt, 1984; Mango, 2000), and these variations have been generally ascribed to several factors, including the type of OM, the characteristics of the branched hydrocarbons and the properties of the sedimentary environment (e.g., buried depth and lithology) (Tannenbaum and Kaplan, 1985a; Craddock et al., 2015; Sessions, 2016). This work suggests that clay-OM complexation is also an important factor affecting the concentrations of the generated branched hydrocarbons, in term of the observation that the iC_4/nC_4 and iC_5/nC_5 ratios for the pyrolysis of OMs are very low whereas those for the Mt-OM complexes are increased significantly. Moreover, the diverse pyrolytic behaviors of different organics reflects the high complexity of the pyrolysis of natural OM. In future work, it would be very meaningful to extract asphaltenes from crude oils from different sources (e.g., different basins and varying thermal maturities) and to use the typical components of the asphaltenes to prepare clay-OM complexes for OM pyrolysis study. The basic information obtained from the pyrolysis behaviors of the different organics with various functional groups would be beneficial to conducting such a study and thereby for understanding the detailed mechanisms of hydrocarbon generation induced by pyrolysis of natural organics. In particular, the finding about the pyrolysis-inhibiting effect of clay, occurred in the case halide-containing organics, exhibits a novel clay-OM reaction, compared to the promoted pyrolysis of organics in the presence of clay that had been generally investigated. This pyrolysis-inhibiting effect works through the promotion of Hoffmann elimination of the halide-containing organics by the catalysis of B acid sites of Mt. In view of that halide-containing organics are widely occurring in some marine-deposited rocks and sediments (Fuge, 1988; Muramatsu et al., 2007), the pyrolysis of the related organics in such rocks deserves extra attention because of the possible pyrolysis-inhibiting effect.

The findings of this work further verify the important role of swelling clay minerals, such as montmorillonite, for OM storage and pyrolysis. As described earlier, the various catalytic sites of clay play multiple roles in OM pyrolysis, which dramatically change the yield and composition

of the produced gaseous hydrocarbons. Particularly, the function of the interlayer space of swelling clay is highlighted. Mt exhibited either a pyrolysis-promoting effect (for the cases of OA and ODA) or a pyrolysis-inhibiting effect (for OTAB). Both effects became much more distinct for the OM existed in the interlayer space of Mt, in another word, the interlayer space of Mt acted like an 'amplifier' that obviously magnified the effect of swelling clay, which is due to the interlayer B acid sites with high acidity. Another reason making the interlayer space of swelling clay be of particular importance is that the interlayer space accounts for the large inner surface area of swelling clay, which are tens of times greater than those of non-swelling clays such as illite (Macht et al., 2011). This feature of swelling clay allows the accommodation of the organics in the interlayer space and thereby the interlayer clay-OM complexation. Due to the ubiquitous occurrence of swelling clays (such as montmorillonite) in source rocks and sedimentary environments, and the wide co-existence of swelling clays and OM in the processes of geological evolution and the carbon cycle (Schmidt et al., 2011; Arndt et al., 2013), future studies need to pay much more attention on the roles of swelling clay minerals in the related geological events.

Mixed-layer illite-smectite (I-S) clay, especially for those with low I/S ratio (high proportion of smectite layers), can be considered a special example of swelling clay, because I-S clay contain smectite layers. I-S clay exists widely in sedimentary rocks and in many cases is more ubiquitous than smectite group minerals or illite (Srodon, 1999). For the interlayer clay-OM complexation, it can be anticipated that the smectite layer of I-S clay might behave like swelling clay minerals, for example, it is also capable of accommodating the organics through ion exchange (Li et al., 2010). However, since the knowledge on the solid acidity of I-S clay (especially about the distribution of solid acidity at smectite or illite layers) is rare up to now, how the complexation between I-S clay and OM affects the OM pyrolysis still remains unknown, and it merits further investigation.

It is noteworthy that, the illitization of smectite occurs commonly during diagenesis and hydrocarbon generation in petroleum basin. The smectite illitization is accompanied by the changes of mineral phases and thereby the minerals microstructure and surface properties. Such an evolution would have several possible impacts on the pyrolysis of OM: (i) the loss of interlayer space during smectite illitization might result in the removal of interlayer OM; (ii) the surface acidity might change. For example, the interlayer B acid sites no longer exist, and the B acidity at the external surface might also dramatically change. According to previous studies (Newman, 1987), the higher Si—Al substitution in SiO_4 tetrahedron of illite than that of smectite might make the basal surface of illite be more negatively charged, which might electrostatically capture H_3O^+ ions that act as B acid sites; (iii) the illitization of smectite might be accompanied with large amounts of intermediate mineral phases, and the related microstructure and properties changes would also strongly affect the forms of clay-OM association and the OM pyrolysis. Ahn et al. (1999) reported a special case of clay-OM complex, in which an interstratified carbonaceous material was formed within a natural illite. This unique clay-OM complex was believed to occur during the illitization of smectite, which had adsorbed organic molecules in its interlayers and eventually evolved toward illite. This observation exemplifies the complexity of the illitization of interlayer clay-OM complexes.

Recently, Li et al. (2016) reported a distinct effect of clay-OM complexation on the illitization occurred in a dark mudstones from the Dongying Depression, China. They found that the smectite illitization in the dark mudstones was delayed due to the pillaring effect of the interlayer OM of smectite above a certain depth (3100 m), whereas the interlayer OM was desorbed and organic acid was formed below 3100 m, which led to the dissolution of smectite layers and the acceleration of illitization. This observation implies that some features of the argillaceous source rocks in petroleum basin, such as the time and space difference (or accordance) and the mutual interactions of different processes above-described, should be taken into account upon applying the present simulation experiment results.

5. CONCLUSIONS

The findings of this work clearly demonstrate that the complexation between OM and clay minerals significantly influences the pyrolysis of OM. The solid acidity of clay minerals and the nature of the OM are the two key factors that strongly affect the yield and composition of the gaseous hydrocarbons produced from the pyrolysis of OM in the clay-OM complexes. B acid sites in the clay mainly promote the cracking of hydrocarbons through a carbocation mechanism and boost the isomerization of normal hydrocarbons. L acid sites promote the decarboxylation of OM that contains carboxyl groups. For the pyrolysis of fatty acids (i.e., OA) and fatty amines (i.e., ODA), clay-OM complexation increases the production of low-molecular-mass gaseous hydrocarbons and CO_2, for which clay minerals primarily act as a catalyst to initiate the hydrocarbon cracking of the OM (i.e., OA and ODA) through the carbocation mechanism. In contrast, clay minerals inhibit the pyrolysis of OM for alkyl quaternary ammonium organic (i.e., OTAB) because of the presence of halide ions in alkyl quaternary ammonium, which reduces the total amount of C_{1-5} hydrocarbons that are produced from pyrolysis. This pyrolysis-inhibiting effect works through the promotion of Hoffmann elimination in the presence of B acid sites in Mt, which releases lower amounts of gas hydrocarbons than the nucleophilic reaction from halide ions in OM. In particular, our results indicated that the interlayer space of swelling clays acts as an 'amplifier' by magnifying the above-mentioned pyrolysis-promoting or pyrolysis-inhibiting effect, because of the B acid sites with high acidity in the interlayer space of Mt. In summary, our findings demonstrate the high dependence of the thermal stability of OM in clay-OM complexes on the surface reactivity of clay minerals and the nature of the OM, which should be taken into account during the investigation on the geochemical processes (e.g., hydrocarbon generation and carbon cycle) in which clay-OM complexes are involved.

ACKNOWLEDGMENTS

This work was financially supported by the National Natural Science Foundation of China (Grant Nos. 41272059, 41472044 and 41173069), the National Basic Research Program of China (Grant No. 2012CB214704-01), Technology Program of Guangzhou (Grant No. 201510010153), Youth Innovation Promotion Association CAS and CAS-SAFEA International Partnership Program for Creative Research Teams (Grant No. 20140491534). This is a contribution (IS-2397) from GIGCAS.

APPENDIX A. SUPPLEMENTARY MATERIAL

Supplementary data associated with this article can be found, in the online version, at http://dx.doi.org/10.1016/j.gca.2017.04.045.

REFERENCES

Ahn J. H., Cho M. and Buseck P. R. (1999) Interstratification of carbonaceous material within illite. *Am. Miner.* **84**(11–12), 1967–1970.

Alomon W. and Johns W. (1975) Petroleum forming reactions: the mechanism and rate of clay catalyzed fatty acid decarboxylation. *Adv. Org. Geochem.* **157**, 170.

Andjelkovic T., Perovic J., Purenovic M., Blagojevic S., Nikolic R., Andjelkovic D. and Bojic A. (2006) A direct potentiometric titration study of the dissociation of humic acid with selectively blocked functional groups. *Eclet. Quim.* **31**(3), 39–46.

Arndt S., Jørgensen B. B., LaRowe D. E., Middelburg J. J., Pancost R. D. and Regnier P. (2013) Quantifying the degradation of organic matter in marine sediments: a review and synthesis. *Earth Sci. Rev.* **123**, 53–86.

Bellucci F., Camino G., Frache A. and Sarra A. (2007) Catalytic charring–volatilization competition in organoclay nanocomposites. *Polym. Degrad. Stab.* **92**(3), 425–436.

Bergamaschi B. A., Tsamakis E., Keil R. G., Eglinton T. I., Montluçon D. B. and Hedges J. I. (1997) The effect of grain size and surface area on organic matter, lignin and carbohydrate concentration, and molecular compositions in Peru Margin sediments. *Geochim. Cosmochim. Acta* **61**(6), 1247–1260.

Bousige C., Ghimbeu C. M., Vix-Guterl C., Pomerantz A. E., Suleimenova A., Vaughan G., Garbarino G., Feygenson M., Wildgruber C., Ulm F. J., Pellenq R. J. M. and Coasne B. (2016) Realistic molecular model of kerogen's nanostructure. *Nat. Mater.* **15**(5), 576–582.

Bergaya F. and Lagaly G. (2013) *Handbook of Clay Science*, second ed. Elsevier, The Netherlands.

Berthonneau J., Grauby O., Abuhaikal M., Pellenq R. J. M., Ulm F. J. and Van Damme H. (2016) Evolution of organo-clay composites with respect to thermal maturity in type II organic-rich source rocks. *Geochim. Cosmochim. Acta* **195**, 68–83.

Craddock P. R., Le Doan T. V., Bake K., Polyakov M., Charsky A. M. and Pomerantz A. E. (2015) Evolution of kerogen and bitumen during thermal maturation via semi-open pyrolysis investigated by infrared spectroscopy. *Energy Fuels* **29**(4), 2197–2210.

Cui L., Khramov D. M., Bielawski C. W., Hunter D. L., Yoon P. J. and Paul D. R. (2008) Effect of organoclay purity and degradation on nanocomposite performance, Part 1: surfactant degradation. *Polymer* **49**(17), 3751–3761.

Davis R. D., Gilman J. W., Sutto T. E., Callahan J. H., Trulove P. C. and de Long H. C. (2004) Improved thermal stability of organically modified layered silicates. *Clays Clay Miner.* **52**(2), 171–179.

Espitalie J., Madec M. and Tissot B. (1980) Role of mineral matrix in kerogen pyrolysis: influence on petroleum generation and migration. *AAPG Bull.* **64**(1), 59–66.

Faure P., Schlepp L., Burkle-Vitzthum V. and Elie M. (2003) Low temperature air oxidation of *n*-alkanes in the presence of Na-smectite. *Fuel* **82**(14), 1751–1762.

Frenkel M. (1974) Surface acidity of montmorillonites. *Clays Clay Miner.* **22**(5–6), 441–465.

Fripiat J. and Cruz-Cumplido M. (1974) Clays as catalysts for natural processes. *Annu. Rev. Earth Planet. Sci.* **2**, 239.

Fuge R. (1988) Sources of halogens in the environment, influences on human and animal health. *Environ. Geochem. Health* **10**(2), 51–61.

Galwey A. K. (1970) Reactions of alcohols and of hydrocarbons on montmorillonite surfaces. *J. Catal.* **19**(3), 330–342.

Galwey A. K. (1972) The rate of hydrocarbon desorption from mineral surfaces and the contribution of heterogeneous catalytic-type processes to petroleum genesis. *Geochim. Cosmochim. Acta* **36**(10), 1115–1130.

Greensfelder B. S., Voge H. H. and Good G. M. (1949) Catalytic and thermal cracking of pure hydrocarbons: mechanisms of reaction. *Ind. Eng. Chem.* **41**(11), 2573–2584.

He H. P., Frost R. L. and Zhu J. X. (2004) Infrared study of HDTMA+ intercalated montmorillonite. *Spectrochim. Acta A Mol. Biomol. Spectrosc.* **60**(12), 2853–2859.

Hedges J. I. and Keil R. G. (1995) Sedimentary organic matter preservation: an assessment and speculative synthesis. *Mar. Chem.* **49**(2–3), 81–115.

Heller-Kallai L., Aizenshtat Z. and Miloslavski I. (1984) The effect of various clay minerals on the thermal decomposition of stearic acid under 'bulk flow' conditions. *Clay Miner.* **19**, 779–788.

Hoering T. (1984) Thermal reactions of kerogen with added water, heavy water and pure organic substances. *Org. Geochem.* **5**(4), 267–278.

Hu M., Cheng Z., Zhang M., Liu M., Song L., Zhang Y. and Li J. (2014) Effect of calcite, kaolinite, gypsum, and montmorillonite on Huadian oil shale kerogen pyrolysis. *Energy Fuels* **28**(3), 1860–1867.

Huizinga B. J., Tannenbaum E. and Kaplan I. R. (1987a) The role of minerals in the thermal alternation of organic matter-iii. Generation of bitumen in laboratory experiments. *Org. Geochem.* **11**(6), 591–604.

Huizinga B. J., Tannenbaum E. and Kaplan I. R. (1987b) The role of minerals in the thermal alternation of organic matter-IV. Generation of *n*-alkanes, acyclic isoprenoids, and alkenes in laboratory experiment. *Geochim. Cosmochim. Acta* **51**, 1083–1097.

Hunt J. M. (1984) Generation and migration of light hydrocarbons. *Science* **226**(4680), 1265–1270.

Ingalls A. E., Aller R. C., Lee C. and Wakeham S. G. (2004) Organic matter diagenesis in shallow water carbonate sediments. *Geochim. Cosmochim. Acta* **68**(21), 4363–4379.

Macht F., Eusterhues K., Pronk G. J. and Totsche K. U. (2011) Specific surface area of clay minerals: comparison between atomic force microscopy measurements and bulk-gas (N_2) and -liquid (EGME) adsorption methods. *Appl. Clay Sci.* **53**(1), 20–26.

Johns W. D. (1979) Clay mineral catalysis and petroleum generation. *Annu. Rev. Earth Planet. Sci.* **7**(1), 183–189.

Johns W. D. and Shimoyama A. (1972) Clay minerals and petroleum-forming reactions during burial and diagenesis. *AAPG Bull.* **56**(11), 2160–2167.

Jurg J. W. and Eisma E. (1964) Petroleum hydrocarbons generation from fatty acid. *Science* **144**(3625), 1451–1452.

Karaca S., Gürses A. and Korucu M. E. (2013) Investigation of the orientation of CTA+ ions in the interlayer of CTAB pillared montmorillonite. *J. Chem.* **3**, 392–399.

Keil R. G. and Cowie G. L. (1999) Organic matter preservation through the oxygen-deficient zone of the NE Arabian Sea as discerned by organic carbon: mineral surface area ratios. *Mar. Geol.* **161**(1), 13–22.

Keil R. G., Tsamakis E., Fuh C. B., Giddings J. C. and Hedges J. I. (1994) Mineralogical and textural controls on the organic composition of coastal marine sediments Hydrodynamic separation using SPLITT-fractionation. *Geochim. Cosmochim. Acta* **58**(2), 879–893.

Kell R. G., Montlucon D. B. and Prahli F. G. (1994) Sorption preservation of labile organic matter in marine sediments. *Nature* **370**(18), 549–551.

Kennedy M. J., Löhr S. C., Fraser S. A. and Baruch E. T. (2014) Direct evidence for organic carbon preservation as clay-organic nanocomposites in a Devonian black shale; from deposition to diagenesis. *Earth Planet. Sci. Lett.* **388**, 59–70.

Kennedy M. J., Pevear D. R. and Hill R. J. (2002) Mineral surface control of organic carbon in black shale. *Science* **295**(5555), 657–660.

Kennedy M. J. and Wagner T. (2011) Clay mineral continental amplifier for marine carbon sequestration in a greenhouse ocean. *Proc. Natl. Acad. Sci.* **108**(24), 9776–9781.

Kissin Y. V. (1987) Catagenesis and composition of petroleum origin of *n*-alkanes and isoalkanes in petroleum crudes. *Geochim. Cosmochim. Acta* **51**(9), 2445–2457.

Krooss B. M., Littke R., Müller B., Frielingsdorf J., Schwochau K. and Idiz E. F. (1995) Generation of nitrogen and methane from sedimentary organic matter: implications on the dynamics of natural gas accumulations. *Chem. Geol.* **126**(3), 291–318.

Kuhl P. E. (1942) Catalytic reforming of hydrocarbon oils. In *U.S. Patent No. 2, 083*. U.S. Patent and Trademark Office, Washington, DC.

Kumar P., Jasra R. V. and Bhat T. S. (1995) Evolution of porosity and surface acidity in montmorillonite clay on acid activation. *Ind. Eng. Chem. Res.* **34**(4), 1440–1448.

Lewan M. D. (1997) Experiments on the role of water in petroleum formation. *Geochim. Cosmochim. Acta* **61**(17), 3691–3723.

Li Y., Cai J., Song M., Ji J. and Bao Y. (2016) Influence of organic matter on smectite illitization: a comparison between red and dark mudstones from the Dongying Depression, China. *Am. Mineral.* **101**(1), 134–145.

Li Z., Jiang W. T., Chen C. J. and Hong H. (2010) Influence of chain lengths and loading levels on interlayer configurations of intercalated alkylammonium and their transitions in rectorite. *Langmuir* **26**(11), 8289–8294.

Li Z., Zhang Z., Sun Y., Lao Y., Lin W. and Wu W. (2003) Catalytic decarboxylations of fatty acids in immature oil source rocks. *Sci. China Ser. D* **46**(12), 1250.

Liu D., Yuan P., Liu H., Cai J., Qin Z., Tan D., Zhou Q., He H. and Zhu J. (2011) Influence of heating on the solid acidity of montmorillonite: a combined study by DRIFT and Hammett indicators. *Appl. Clay Sci.* **52**(4), 358–363.

Liu X., Lu X., Wang R., Zhou H. and Xu S. (2007) Interlayer structure and dynamics of alkylammonium intercalated smectites with and without water: a molecular dynamics study. *Clays Clay Miner.* **55**(6), 554–564.

Liu X., Lu X., Sprik M., Cheng J., Meijer E. J. and Wang R. (2013) Acidity of edge surface sites of montmorillonite and kaolinite. *Geochim. Cosmochim. Acta* **117**(5), 180–190.

Liu X., Cheng J., Sprik M., Lu X. and Wang R. (2014) Surface acidity of 2:1-type dioctahedral clay minerals from first principles molecular dynamics simulations. *Geochim. Cosmochim. Acta* **140**(140), 410–417.

Liu X., Lu X., Cheng J., Sprik M. and Wang R. (2015a) Temperature dependence of interfacial structures and acidity of clay edge surfaces. *Geochim. Cosmochim. Acta* **160**, 91–99.

Liu X., Cheng J., Sprik M., Lu X. and Wang R. (2015b) Interfacial structures and acidity of edge surfaces of ferruginous smectites. *Geochim. Cosmochim. Acta* **168**(3), 293–301.

Lopez-Sangil L. and Rovira P. (2013) Sequential chemical extractions of the mineral-associated soil organic matter: an integrated approach for the fractionation of organo-mineral complexes. *Soil Biol. Biochem.* **62**, 57–67.

Lu X. C., Hu W. X., Fu Q., Miao D. Y., Zhou G. J. and Hong Z. H. (1999) Study of combination pattern of soluble organic matters and clay minerals in the immature source rocks in Dongying depression, China. *Scientia Geologica Sinica* **34**, 72–80 (in Chinese).

Ma Y. H., Zhu J. X., He H. P., Yuan P., Shen W. and Liu D. (2010) Infrared investigation of organo-montmorillonites prepared from different surfactants. *Spectrochim. Acta A Mol. Biomol. Spectrosc.* **76**(2), 122–129.

Madejova J. and Komadel P. (2001) Baseline studies of the clay minerals society source clays: infrared methods. *Clays Clay Miner.* **49**(5), 410–432.

Mango F. D. (1996) Transition metal catalysis in the generation of natural gas. *Org. Geochem.* **24**(10), 977–984.

Mango F. D. (2000) The origin of light hydrocarbons. *Geochim. Cosmochim. Acta* **64**(7), 1265–1277.

Mayer L. M. (1994) Surface area control of organic carbon accumulation in continental shelf sediments. *Geochim. Cosmochim. Acta* **58**(4), 1271–1284.

Mayer L. M. (1999) Extent of coverage of mineral surfaces by organic matter in marine sediments. *Geochim. Cosmochim. Acta* **63**(2), 207–215.

Mayer L. M. (2004) The inertness of being organic. *Mar. Chem.* **92** (1–4), 135–140.

Muramatsu Y., Doi T., Tomaru H., Fehn U., Takeuchi R. and Matsumoto R. (2007) Halogen concentrations in pore waters and sediments of the Nankai Trough, Japan: implications for the origin of gas hydrates. *Appl. Geochem.* **22**(3), 534–556.

Newman A. C. (1987) *Chemistry of clays and clay minerals*. Longman Scientific and Technical.

Pálková H., Madejová J., Zimowska M. and Serwicka E. M. (2010) Laponite-derived porous clay heterostructures: II. FTIR study of the structure evolution. *Microporous Mesoporous Mater.* **127** (3), 237–244.

Pan C. C., Geng A. S., Zhong N. N., Liu J. Z. and Yu L. P. (2008) Kerogen pyrolysis in the presence and absence of water and minerals. 1. Gas components. *Energy Fuels* **22**(1), 416–427.

Pan C. C., Jiang L. L., Liu J. Z., Zhang S. C. and Zhu G. Y. (2010) The effects of calcite and montmorillonite on oil cracking in confined pyrolysis experiments. *Org. Geochem.* **41**(7), 611–626.

Perez Rodriguez J. L., Weiss A. and Lagaly G. (1977) A natural clay organic complex from Andalusian black earth. *Clays Clay Miner.* **25**(3), 243–251.

Qader S. and Hill G. R. (1969) Hydrocracking of gas oil. *Ind. Eng. Chem. Process Des. Dev.* **8**(1), 98–105.

Rajagopal S., Grimm T. L., Collins D. J. and Miranda R. (1992) Denitrogenation of piperidine on alumina, silica, and silica-aluminas the effect of surface acidity. *J. Catal.* **137**(2), 453–461.

Ransom B., Kim D., Kastner M. and Wainwright S. (1998) Organic matter preservation on continental slopes importance of mineralogy and surface area. *Geochim. Cosmochim. Acta* **62** (8), 1329–1345.

Rupert J., Granquist W. and Pinnavaia T. (1987) Catalytic properties of clay minerals. *Monogr. Mineral. Soc.* **6**, 275–318.

Salmon V., Derenne S., Lallier-Verges E., Largeau C. and Beaudoin B. (2000) Protection of organic matter by mineral matrix in a Cenomanian black shale. *Org. Geochem.* **31**(5), 463–474.

Satterberg J., Arnarson T. S., Lessard E. J. and Keil R. G. (2003) Sorption of organic matter from four phytoplankton species to montmorillonite, chlorite and kaolinite in seawater. *Mar. Chem.* **81**(1–2), 11–18.

Scaffaro R., Mistretta M. C., La Mantia F. P. and Frache A. (2009) Effect of heating of organo-montmorillonites under different atmospheres. *Appl. Clay Sci.* **45**(4), 185–193.

Schmidt M. W., Torn M. S., Abiven S., Dittmar T., Guggenberger G., Janssens I. A., Kleber M., Kogel-Knabner I., Lehmann J., Manning D. A., Nannipieri P., Rasse D. P., Weiner S. and Trumbore S. E. (2011) Persistence of soil organic matter as an ecosystem property. *Nature* **478**(7367), 49–56.

Schulten H. R., Leinweber P. and Theng B. K. G. (1996) Characterization of organic matter in an interlayer clay-organic complex from soil by pyrolysis methylation-mass spectrometry. *Geoderma* **69**(1), 105–118.

Seewald J. S., Benitez-Nelson B. C. and Whelan J. K. (1998) Laboratory and theoretical constraints on the generation and composition of natural gas. *Geochim. Cosmochim. Acta* **62**(9), 1599–1617.

Seewald J. S. (2003) Organic–inorganic interactions in petroleum-producing sedimentary basins. *Nature* **426**(6964), 327–333.

Sessions A. L. (2016) Factors controlling the deuterium contents of sedimentary hydrocarbons. *Org. Geochem.* **96**, 43–64.

Shimoyama A. and Johns W. D. (1971) Catalytic conversion of fatty acids to petroleum-like paraffins and their maturation. *Nature* **232**(33), 140–144.

Singh B., Patial J., Sharma P., Agarwal S. G., Qazi G. N. and Maity S. (2007) Influence of acidity of montmorillonite and modified montmorillonite clay minerals for the conversion of longifolene to isolongifolene. *J. Mol. Catal. A: Chem.* **266**(1–2), 215–220.

Slosiariková H., Bujdák J. and Hlavatý V. (1992) Ir spectra of octadecylammonium-montmorillonite in the range of the si-o vibrations. *J. Inclusion Phenom. Mol. Recognit. Chem.* **13**(3), 267–272.

Solomon D. H. (1968) Clay minerals as electron acceptors and/or electron donors in organic reactions. *Clays Clay Miner.* **16**(31), 2160–2167.

Srodon J. (1999) Nature of mixed-layer clays and mechanisms of their formation and alteration. *Annu. Rev. Earth Planet. Sci.* **27** (1), 19–53.

Tannenbaum E. and Kaplan I. R. (1985a) Role of minerals in the thermal alteration of organic matter-I: generation of gases and condensates under dry condition. *Geochim. Cosmochim. Acta* **49** (12), 2589–2604.

Tannenbaum E. and Kaplan I. R. (1985b) Low Mr hydrocarbons generated during hydrous and dry pyrolysis of kerogen. *Nature* **317**(24), 708–709.

Theng B. K. G. (1971) Mechanisms of formation of colored clay–organic complexes. A review. *Clays Clay Miner.* **19**(6), 383–390.

Theng B. K. G., Churchman G. J. and Newman R. H. (1986) The occurrence of interlayer clay-organic complexes in two New Zealand soils. *Soil Sci.* **142**(5), 262–266.

Thiel V., Jenisch A., Wörheide G., Löwenberg A., Reitner J. and Michaelis W. (1999) Mid-chain branched alkanoic acids from "living fossil" demosponges a link to ancient sedimentary lipids. *Org. Geochem.* **30**(1), 1–14.

Thompson K. F. M. (1979) Light hydrocarbons in subsurface sediments. *Geochim. Cosmochim. Acta* **43**(5), 657–672.

Thompson K. F. M. (2016) Hybrid gas condensates and the evolution of their volatile light hydrocarbons. *Org. Geochem.* **93**, 32–50.

Tournassat C., Davis J. A., Chiaberge C., Grangeon S. and Bourg I. C. (2016) Modeling the acid-base properties of montmorillonite edge surfaces. *Environ. Sci. Technol.* **50**(24), 13436–13445.

Tyagi B., Chudasama C. D. and Jasra R. V. (2006) Characterization of surface acidity of an acid montmorillonite activated with hydrothermal, ultrasonic and microwave techniques. *Appl. Clay Sci.* **31**(1–2), 16–28.

Vandenbroucke M. and Largeau C. (2007) Kerogen origin, evolution and structure. *Org. Geochem.* **38**(5), 719–833.

Wei Z., Moldowan J. M. and Paytan A. (2006) Diamondoids and molecular biomarkers generated from modern sediments in the absence and presence of minerals during hydrous pyrolysis. *Org. Geochem.* **37**(8), 891–911.

Xiang M. J., Shi J., Zhou Y. and Qu D. (1997) The distribution and evolution of fatty acids in various sediments and its significance. *Acta Sedimentol. Sin.* **15**(2), 84–88 (in Chinese).

Xie W., Gao Z., Pan W. P., Hunter D., Singh A. and Vaia R. (2001) Thermal degradation chemistry of alkyl quaternary ammonium montmorillonite. *Chem. Mater.* **13**(9), 2979–2990.

Yariv S., Borisover M. and Lapides I. (2011) Few introducing comments on the thermal analysis of organoclays. *J. Therm. Anal. Calorim.* **105**(3), 897–906.

Yuan P., Annabi-Bergaya F., Tao Q., Fan M. D., Liu Z. W., Zhu J. X., He H. P. and Chen T. (2008) A combined study by XRD, FTIR, TG and HRTEM on the structure of delaminated Fe-intercalated/pillared clay. *J. Colloid Interface Sci.* **324**(1–2), 142–149.

Zhu X., Cai J., Liu W. and Lu X. (2016) Occurrence of stable and mobile organic matter in the clay-sized fraction of shale: significance for petroleum geology and carbon cycle. *Int. J. Coal Geol.* **160–161**, 1–10.

Zimmerman A. R., Goyne K. W., Chorover J., Komarneni S. and Brantley S. L. (2004) Mineral mesopore effects on nitrogenous organic matter adsorption. *Org. Geochem.* **35**(3), 355–375.

Associate editor: Hailiang Dong